Supporting Information

Periodicity and Global Order Parameter of Hexagonally Packed Cylinders in a Periodic Box

Yuan Feng[1], *Jiaping Wu*[1], *Baohui Li*[1,*], *and Qiang Wang*[2,*]

[1]School of Physics, Nankai University

No. 94 Weijin Rd., Nankai District, Tianjin 300071, P. R. China

[2]Department of Chemical and Biological Engineering, Colorado State University

1370 Campus Delivery, Fort Collins, CO 80523-1370, USA

1. Complete Derivation in Sec. 2.2 of the Main Text

Here we follow the notation and numbering of equations in Sec. 2.2 of the main text to complete our derivation. From $\mathbf{a}_1 = Lx_1\mathbf{e}_{x'} + Ly_1\mathbf{e}_{y'}$ and $\mathbf{a}_2 = L\left(x_1/2 - \sqrt{3}y_1/2\right)\mathbf{e}_{x'} + L\left(\sqrt{3}x_1/2 + y_1/2\right)\mathbf{e}_{y'}$, we obtain

$$\mathbf{e}_{x'} = \frac{1}{\sqrt{3}L}\left[\left(\sqrt{3}x_1 + y_1\right)\mathbf{a}_1 - 2y_1\mathbf{a}_2\right], \tag{S1}$$

$$\mathbf{e}_{y'} = \frac{1}{\sqrt{3}L}\left[\left(-x_1 + \sqrt{3}y_1\right)\mathbf{a}_1 + 2x_1\mathbf{a}_2\right]. \tag{S2}$$

We also obtain with the law of cosine $x_1 = \mathbf{b}'_x \bullet \mathbf{a}_1 / |\mathbf{b}'_x||\mathbf{a}_1| = \left(2m_{1,x} + m_{2,x}\right)/2a_{m,x}$, and $y_1 = -\sqrt{1 - x_1^2} = -\sqrt{3}m_{2,x}/2a_{m,x}$; substituting them into Eqs. (S1) and (S2) then gives

$$\mathbf{e}_{x'} = \frac{m_{1,x}\mathbf{a}_1 + m_{2,x}\mathbf{a}_2}{La_{m,x}}, \tag{S3}$$

* To whom correspondence should be addressed. E-mail: baohui@nankai.edu.cn (BL), q.wang@colostate.edu (QW).

$$\mathbf{e}_{y'} = \frac{-\left(m_{1,x}+2m_{2,x}\right)\mathbf{a}_1 + \left(2m_{1,x}+m_{2,x}\right)\mathbf{a}_2}{\sqrt{3}La_{m,x}}. \tag{S4}$$

Substituting Eqs. (S3) and (S4) into Eq. (11) gives

$$\mathbf{b}'_y = -L_y \frac{\left[\sqrt{3}m_{1,x}\sin\alpha_x\sin\alpha_y + \left(m_{1,x}+2m_{2,x}\right)\cos\alpha_x\right]\mathbf{a}_1 + \left[\sqrt{3}m_{2,x}\sin\alpha_x\sin\alpha_y - \left(2m_{1,x}+m_{2,x}\right)\cos\alpha_x\right]\mathbf{a}_2}{\sqrt{3}La_{m,x}},$$

from which we obtain $\begin{cases} m_{1,y} = -L_y \dfrac{\sqrt{3}m_{1,x}\sin\alpha_x\sin\alpha_y + \left(m_{1,x}+2m_{2,x}\right)\cos\alpha_x}{\sqrt{3}La_{m,x}} \le -1 \\ m_{2,y} = -L_y \dfrac{\sqrt{3}m_{2,x}\sin\alpha_x\sin\alpha_y - \left(2m_{1,x}+m_{2,x}\right)\cos\alpha_x}{\sqrt{3}La_{m,x}} \end{cases}$, or equivalently,

$$\frac{L_y}{L}\cos\alpha_x = \frac{\sqrt{3}\bar{m}_{xy}}{2a_{m,x}}, \tag{S5}$$

$$\frac{L_y}{L}\sin\alpha_x\sin\alpha_y = -\frac{m_{xy}}{2a_{m,x}}, \tag{S6}$$

where $\bar{m}_{xy} \equiv m_{1,x}m_{2,y} - m_{2,x}m_{1,y}$ and $m_{xy} \equiv \left(2m_{1,x}+m_{2,x}\right)m_{1,y} + \left(m_{1,x}+2m_{2,x}\right)m_{2,y}$ are integers.

Similarly, substituting Eqs. (S3) and (S4) into Eq. (12) gives

$$\mathbf{b}'_z = -L_z \frac{\left[\sqrt{3}m_{1,x}\cos\alpha_x\sin\alpha_y - \left(m_{1,x}+2m_{2,x}\right)\sin\alpha_x\right]\mathbf{a}_1 + \left[\sqrt{3}m_{2,x}\cos\alpha_x\sin\alpha_y + \left(2m_{1,x}+m_{2,x}\right)\sin\alpha_x\right]\mathbf{a}_2}{\sqrt{3}La_{m,x}},$$

from which we obtain $\begin{cases} m_{1,z} = -L_z \dfrac{\sqrt{3}m_{1,x}\cos\alpha_x\sin\alpha_y - \left(m_{1,x}+2m_{2,x}\right)\sin\alpha_x}{\sqrt{3}a_{m,x}L} \\ m_{2,z} = -L_z \dfrac{\sqrt{3}m_{2,x}\cos\alpha_x\sin\alpha_y + \left(2m_{1,x}+m_{2,x}\right)\sin\alpha_x}{\sqrt{3}a_{m,x}L} \le 0 \end{cases}$, or equivalently,

$$\frac{L_z}{L}\sin\alpha_x = -\frac{\sqrt{3}\bar{m}_{xz}}{2a_{m,x}}, \tag{S7}$$

$$\frac{L_z}{L}\cos\alpha_x\sin\alpha_y = -\frac{m_{xz}}{2a_{m,x}}, \tag{S8}$$

where $\bar{m}_{xz} \equiv m_{1,x}m_{2,z} - m_{2,x}m_{1,z}$ and $m_{xz} \equiv \left(2m_{1,x}+m_{2,x}\right)m_{1,z} + \left(m_{1,x}+2m_{2,x}\right)m_{2,z}$ are integers.

Finally, with $\cos^2\alpha_x+\sin^2\alpha_x=1$, we obtain from Eqs. (S5) and (S7) the constraint

$$\left(\frac{\bar{m}_{xy}}{L_y/L}\right)^2+\left(\frac{\bar{m}_{xz}}{L_z/L}\right)^2=\frac{4a_{m,x}{}^2}{3} \tag{S9}$$

and from Eqs. (S6) and (S8) the constraint

$$\left(\frac{m_{xy}}{L_y/L}\right)^2+\left(\frac{m_{xz}}{L_z/L}\right)^2=4a_{m,x}{}^2\sin^2\alpha_y\,. \tag{S10}$$

According to the above, we therefore have three cases depending on the values of p_x and p_y: In the case of α_y=0 (*i.e.*, p_x=0), we obtain from Eq. (S6) $m_{xy}=0 \;\Rightarrow\; m_{2,y}=-m_{1,y}\left(2m_{1,x}+m_{2,x}\right)\big/\left(m_{1,x}+2m_{2,x}\right)$ and from Eq. (S8) $m_{xz}=0 \;\Rightarrow\; m_{2,z}=-m_{1,z}\left(2m_{1,x}+m_{2,x}\right)\big/\left(m_{1,x}+2m_{2,x}\right)$; substituting them into Eqs. (S5) and (S7), respectively, gives

$$\frac{L_y}{L}\cos\alpha_x=-\sqrt{3}a_{m,x}\frac{m_{1,y}}{m_{1,x}+2m_{2,x}}\,, \tag{S11}$$

$$\frac{L_z}{L}\sin\alpha_x=\sqrt{3}a_{m,x}\frac{m_{1,z}}{m_{1,x}+2m_{2,x}}\,. \tag{S12}$$

Therefore, for given (integer) values of four design parameters $m_{1,x}\geq 1$, $m_{2,x}\geq 0$, $m_{1,y}\leq -1$ and $m_{1,z}\geq 1$, one can obtain the values of $a_{m,x}$, $m_{2,y}\geq 1$ and $m_{2,z}\leq -1$ (the last two must also be integers, thus limiting the values of the four design parameters). One can then obtain $L_x/L=a_{m,x}$ from Eq. (14). By further choosing freely the value of $\alpha_x\in[0,-\pi/2)$, one can finally obtain the values of L_y/L and L_z/L from Eqs. (S11) and (S12), respectively; in the special case of α_x=0 (*i.e.*, p_y=0), $L_z/L>0$ can also be chosen freely.

In the case of α_x=0, we obtain from Eq. (S6) $m_{xy}=0$ thus $m_{2,y}=-m_{1,y}\left(2m_{1,x}+m_{2,x}\right)\big/\left(m_{1,x}+2m_{2,x}\right)$ and from Eq. (S7) $\bar{m}_{xz}=0$ thus $m_{2,z}=m_{2,x}m_{1,z}/m_{1,x}$; substituting them into Eqs. (S5) and (S8), respectively, gives Eq. (S11) and

$$\frac{L_z}{L}\sin\alpha_y=-a_{m,x}\frac{m_{1,z}}{m_{1,x}}\,. \tag{S13}$$

Therefore, for given (integer) values of four design parameters $m_{1,x}\geq 1$, $m_{2,x}\geq 0$, $m_{1,y}\leq -1$ and $m_{1,z}\leq -1$, one can obtain the values of $a_{m,x}$, $m_{2,y}\geq 1$ and $m_{2,z}\leq 0$ (the last two must also be integers, thus limiting the values of the four design parameters). One can then obtain the value of L_y/L from Eq. (S11). By further choosing freely the value of $\alpha_y \in [0,\pi/2)$, one can finally obtain the values of L_x/L and L_z/L from Eqs. (14) and (S13), respectively; in the special case of $\alpha_y=0$, $L_z/L>0$ can also be chosen freely as aforementioned.

In the case of $\alpha_x\neq 0$ and $\alpha_y\neq 0$ (*i.e.*, $p_x>0$ and $p_y>0$), Eqs. (S5) and (S6) give $\bar{m}_{xy}\geq 1$ and $m_{xy}\leq -1$, respectively, and Eqs. (S7) and (S8) give $\bar{m}_{xz}\leq -1$ and $m_{xz}\leq -1$, respectively; these four constraints limit the (integer) values of the six design parameters $m_{1,x}\geq 1$, $m_{2,x}\geq 0$, $m_{1,y}\leq -1$, $m_{2,y}$, $m_{1,z}$ and $m_{2,z}\leq 0$. One can then obtain the value of $a_{m,x}$. Furthermore, Eqs. (S5) and (S6) give $\tan\alpha_x \sin\alpha_y = -m_{xy}\big/\sqrt{3}\bar{m}_{xy}$, and Eqs. (S7) and (S8) give $\tan\alpha_x\big/\sin\alpha_y = \sqrt{3}\bar{m}_{xz}\big/m_{xz}$; from these one can obtain $\tan\alpha_x = \sqrt{-m_{xy}\bar{m}_{xz}/\bar{m}_{xy}m_{xz}}$ and $\sin\alpha_y = \sqrt{-m_{xy}m_{xz}/3\bar{m}_{xy}\bar{m}_{xz}}$, thus $\sin\alpha_x = \sqrt{1\big/\left(1-\bar{m}_{xy}m_{xz}/m_{xy}\bar{m}_{xz}\right)}$ and $\cos\alpha_y = \sqrt{1+m_{xy}m_{xz}/3\bar{m}_{xy}\bar{m}_{xz}}$. One can finally obtain the values of L_x/L, L_y/L and L_z/L from Eqs. (14), (S6) and (S7), respectively.

2. Dissipative Particle Dynamics (DPD) Simulations

Here we follow the notation in our main text, and give the details of our DPD model and simulations used there. The chain connectivity is described by the discrete Gaussian chain model with an effective bond length b; the bonded potential of the k^{th} chain is given by $\beta u_k^{\text{b}} = \frac{3}{2b^2}\sum_{s=1}^{N-1}\left(\mathbf{R}_{k,s+1}-\mathbf{R}_{k,s}\right)^2$, where $\beta\equiv 1/k_BT$ with k_B being the Boltzmann constant and T the thermodynamic temperature, N is the number of segments on each chain, and $\mathbf{R}_{k,s}$ denotes the spatial position of the s^{th} segment on the k^{th} chain. As for the non-bonded interactions, all segments (regardless of their type) repel each other with the pair potential $u^{\kappa}(r) = u_0(r)/\kappa\rho_0$, where r

denotes the distance (under the periodic boundary conditions) between two segments, $\beta u_0(r) = \left(15/2\pi\sigma^3\right)\left(1-r/\sigma\right)^2$ for $r<\sigma$ and 0 otherwise is the normalized DPD potential (*i.e.*, $\int \mathrm{d}\mathbf{r}\beta u_0(r) = 1$), and the generalized Helfand compressibility parameter $\kappa \geq 0$ controls the repulsion strength ($\kappa=0$ corresponds to the hard-sphere chains). In addition, an A segment repels a B segment via the pair potential $u^{\chi}(r) = u_0(r)\chi/\rho_0$ with the generalized Flory-Huggins parameter $\chi \geq 0$ controlling the A-B repulsion strength. In addition to the conservative force due to the above bonded and non-bonded potentials, a (dimensionless) dissipative force $\beta\sigma\mathbf{F}_{jj'}^D = -\gamma\omega^D(r_{jj'})\left[\hat{\mathbf{r}}_{jj'}\bullet\sqrt{\beta m_s}\left(\mathbf{v}_j - \mathbf{v}_{j'}\right)\right]\hat{\mathbf{r}}_{jj'}$ and a (dimensionless) random force $\beta\sigma\mathbf{F}_{jj'}^R = \sqrt{2\gamma\omega^D(r_{jj'})}\xi_{jj'}\hat{\mathbf{r}}_{jj'}$ are also applied on segment j by $j'\neq j$, where $\gamma \geq 0$ is a dimensionless parameter controlling their strength, $\omega^D(r)$ is a dimensionless weight function, $r_{jj'}\equiv|\mathbf{r}_{jj'}|$, $\mathbf{r}_{jj'}\equiv\mathbf{r}_j-\mathbf{r}_{j'}$, $\mathbf{r}_j$ denotes the spatial position of segment j, $\hat{\mathbf{r}}_{jj'} \equiv \mathbf{r}_{jj'}/r_{jj'}$, m_s denotes the mass of each segment, $\mathbf{v}_j$ denotes the velocity of segment j, and $\xi_{jj'}$ is a random number with zero mean and unit variance.

Our DPD simulations are performed on NVIDIA GeForce RTX 3080 GPU using the GALAMOST software package[1]. We use the modified velocity-Verlet algorithm proposed by Groot and Madden[2] (with their parameter λ=0.65) to integrate the Newton's equations of motion, and set γ=6.75, $\omega^D(r)=(1-r/\sigma)^2$ and the integration time step $\delta t = 0.01\sigma\sqrt{\beta m_s}$. For each cubic box of given length L_d, we start the DPD simulation from a randomly generated initial configuration, and equilibrate the system till the mean square chain end-to-end distance and radius of gyration, as well as the global order parameter Ψ for hexagonally packed cylinders (defined in Sec. 4 of the main text), calculated for each collected configuration all reach a plateau.

3. Calculation of the Scaling Factor in Our Global Order Parameter

Ideally, an order parameter for a periodic ordered morphology (POM) should vary between

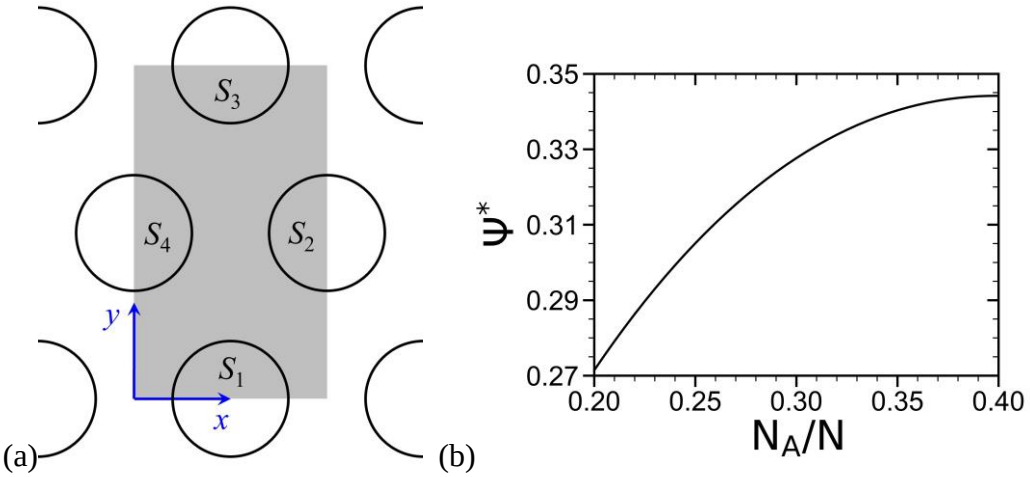

Figure S1: (a) RHP cylinders (represented by circles) in a plane perpendicular to them, where the shaded rectangle has lengths L_x=L and $L_y = \sqrt{3}L$ with L being the intercylinder distance, and S_j (j=1,…,4) denote the four half-circles within the rectangle. (b) The scaling factor Ψ^* calculated for RHP cylinders formed by an incompressible melt of diblock copolymers A-B in the SSL under the mean-field approximation *vs.* the volume fraction of A segments N_A/N.

0 for the (homogeneous) disordered phase and 1 for the POM in the strong-segregation limit (SSL). Here we follow the notation in our main text and calculate the scaling factor Ψ^*, which is taken as the maximum of $\psi^* \equiv \frac{1}{3n_cN}\sum_{i=1}^{3}\left|\sum_{k=1}^{n_c}\left[\sum_{s=1}^{N_A}\exp\left(-\sqrt{-1}\mathbf{q}_i\bullet\mathbf{R}_{k,s}\right)-\sum_{s=N_A+1}^{N}\exp\left(-\sqrt{-1}\mathbf{q}_i\bullet\mathbf{R}_{k,s}\right)\right]\right|$ over all orientations for regular-hexagonally packed (RHP) cylinders formed by an incompressible melt (where $N/\kappa\to\infty$) of diblock copolymers A-B in the SSL (where $\chi N\to\infty$) under the mean-field approximation (where $\rho_0\sigma^3\to\infty$ with all fluctuation/correlation effects neglected). In this case, we can reduce the problem to 2D (*i.e.*, in the plane perpendicular to the cylinders) by considering the (periodic) shaded rectangle of lengths L_x=L and $L_y = \sqrt{3}L$ shown in Fig. S1(a) and obtain $\psi^* = \frac{1}{3L_xL_y}\sum_{i=1}^{3}\left|\int_0^{L_x}dx\int_0^{L_y}dy\left(2\phi_A(\mathbf{r})-1\right)\exp\left(-\sqrt{-1}\mathbf{q}_i\bullet\mathbf{r}\right)\right|$, where the volume fraction of A segments

$\phi_{\rm A}(\mathbf{r}) \equiv \frac{V}{n_c N}\sum_{k=1}^{n_c}\sum_{s=1}^{N_{\rm A}}\delta(\mathbf{r}-\mathbf{R}_{k,s}) = 1$ at spatial position **r** inside any of the four half-circles S_j (j=1,…,4) of radius $R = \sqrt{\sqrt{3}N_{\rm A}/2\pi N}L$ in the rectangle and 0 otherwise (such that $\frac{1}{L_x L_y}\int_0^{L_x}{\rm d}x\int_0^{L_y}{\rm d}y\phi_{\rm A}(\mathbf{r}) = \frac{N_{\rm A}}{N}$); with $\mathbf{q}_1 = 2\pi\left(1/L_x, 1/L_y, 0\right)^T$, $\mathbf{q}_2 = 2\pi\left(1/L_x, -1/L_y, 0\right)^T$ and $\mathbf{q}_3 = 2\pi\left(0, 2/L_y, 0\right)^T$, we then obtain after some algebra $\Psi^* = \frac{2}{3L_x L_y}\sum_{i=1}^{3}\sqrt{\left[\sum_{j=1}^{4}\int_{S_j}{\rm d}x{\rm d}y\cos\left(\mathbf{q}_i\bullet\mathbf{r}\right)\right]^2 + \left[\sum_{j=1}^{4}\int_{S_j}{\rm d}x{\rm d}y\sin\left(\mathbf{q}_i\bullet\mathbf{r}\right)\right]^2}$; with $\int_{S_2}{\rm d}x{\rm d}y\sin\left(\mathbf{q}_3\bullet\mathbf{r}\right) = \int_{S_4}{\rm d}x{\rm d}y\sin\left(\mathbf{q}_3\bullet\mathbf{r}\right) = 0$, we then calculate all other integrals over the area S_j numerically using the Romberg integration[3]. Fig. S1(b) shows that $\Psi^*\approx 0.3276$ at $N_{\rm A}/N$=0.3 and increases with increasing $N_{\rm A}/N$.

References:

1. Y. L. Zhu, H. Liu, Z. W. Li, H. J. Qian, G. Milano and Z. Y. Lu, J. Comput. Chem. **34** (25), 2197-2211 (2013).
2. R. D. Groot and T. J. Madden, J. Chem. Phys. **108** (20), 8713-8724 (1998).
3. W. H. Press, Chap. 4.3 in *Numerical recipes in C: The art of scientific computing* (Cambridge University Press, Cambridge; New York, 1992).